nature neuroscience

Mitochondrial CB_1 receptors regulate neuronal energy metabolism

Giovanni Bénard[1–3,11], Federico Massa[1,3,11], Nagore Puente[4], Joana Lourenço[1,3,5,10], Luigi Bellocchio[1,3], Edgar Soria-Gómez[1,3], Isabel Matias[1,3], Anna Delamarre[1,3], Mathilde Metna-Laurent[1,3], Astrid Cannich[1,3], Etienne Hebert-Chatelain[1,3], Christophe Mulle[3,5], Silvia Ortega-Gutiérrez[6], Mar Martín-Fontecha[6], Matthias Klugmann[7,8], Stephan Guggenhuber[7], Beat Lutz[7], Jürg Gertsch[9], Francis Chaouloff[1,3], María Luz López-Rodríguez[6], Pedro Grandes[4], Rodrigue Rossignol[2,3] & Giovanni Marsicano[1,3]

The mammalian brain is one of the organs with the highest energy demands, and mitochondria are key determinants of its functions. Here we show that the type-1 cannabinoid receptor (CB_1) is present at the membranes of mouse neuronal mitochondria ($mtCB_1$), where it directly controls cellular respiration and energy production. Through activation of $mtCB_1$ receptors, exogenous cannabinoids and *in situ* endocannabinoids decreased cyclic AMP concentration, protein kinase A activity, complex I enzymatic activity and respiration in neuronal mitochondria. In addition, intracellular CB_1 receptors and mitochondrial mechanisms contributed to endocannabinoid-dependent depolarization-induced suppression of inhibition in the hippocampus. Thus, $mtCB_1$ receptors directly modulate neuronal energy metabolism, revealing a new mechanism of action of G protein–coupled receptor signaling in the brain.

The brain represents only 2% of the total body weight in mammals, but it consumes up to 20% of the body's resting energy production[1,2]. Ensuring and regulating cellular energy supplies, mitochondria are key elements of eukaryotic cell functions[1,3] that are crucial for the regulation of brain functions[1,4]. The involvement of neuronal energetics in brain physiology and pathology is the focus of intensive research[1,4,5], but the molecular mechanisms linking mitochondrial activity to brain functions are still poorly documented.

G protein–coupled receptors (GPCRs) represent one of the largest protein families controlling neuronal activity. The presence of GPCRs on neuronal mitochondria and their potential ability to modulate neuronal energetics and function is still a matter of speculation[6]. However, there is now consistent evidence that mitochondria contain G proteins[7,8]. Moreover, several reports have shown the intramitochondrial localization of potential downstream effectors of G protein signaling, such as soluble adenylyl cyclase[9], phosphodiesterase[10,11] and protein kinase A (PKA)[12]. Thus, cAMP can be produced in mitochondria, leading to activation of PKA and phosphorylation of mitochondrial proteins, eventually regulating mitochondrial respiration and energy production[10,11,13,14]. However, the upstream mechanisms regulating the intramitochondrial cAMP–PKA signaling cascade in neurons, and the mechanisms coupling mitochondrial activity and neuronal physiology, remain poorly understood[1,4].

CB_1 receptors are GPCRs highly enriched in neuronal plasma membranes, where they tightly control neuronal activity, metabolism and functions[15–17]. Early studies suggested that the *Cannabis sativa* (marijuana)-derivative cannabinoid Δ^9-tetrahydrocannabinol (THC) could affect mitochondrial functions[18]. However, with the identification of cannabinoid receptors as typical plasma membrane GPCRs[15,19], mitochondrial effects of lipophilic cannabinoids on neurons were ascribed to nonspecific alterations of membrane properties[20]. Recent evidence points also to the ability of CB_1 receptor signaling to regulate mitochondrial biogenesis in peripheral non-neural tissues[21,22]. The lipophilic nature of most cannabinoids[15] implies that receptor–ligand interactions might occur not only at plasma membranes, but also inside cells. Indeed, different intracellular compartments contribute to the regulation of endocannabinoid metabolism[23,24], and CB_1 receptors have been shown to functionally signal in lysosomal or endosomal intracellular membranes[25].

The present study stemmed from the neuroanatomical observation that CB_1 receptor immunogold particles are often detected on neuronal mitochondria in electron microscopy experiments, but they are generally considered nonspecific background labeling. This observation prompted us to investigate the specificity of this signal by using mutant mice constitutively lacking the CB_1 receptor[26]. The results showed that CB_1 receptors are present on neuronal mitochondrial

[1]INSERM, Neurocentre Magendie, Physiopathologie de la plasticité neuronale, Endocannabinoids and Neuroadaptation, U862, Bordeaux, France. [2]Université de Bordeaux, Maladies Rares: Génétique et Métabolisme (MRGM), EA 4576, Bordeaux, France. [3]Université de Bordeaux, Neurocentre Magendie, Physiopathologie de la plasticité neuronale, U862, Bordeaux, France. [4]Department of Neurosciences, Faculty of Medicine and Dentistry, University of the Basque Country UPV/EHU, Leioa, Spain. [5]Laboratoire Physiologie Cellulaire de la Synapse, Centre National de la Recherche Scientifique UMR 5091, Bordeaux, France. [6]Department of Organic Chemistry, Complutense University, Madrid, Spain. [7]Institute of Physiological Chemistry, University Medical Center of the Johannes Gutenberg University, Mainz, Germany. [8]Translational Neuroscience Facility, Department of Physiology, School of Medical Sciences, University of New South Wales, Sydney, New South Wales, Australia. [9]Institute of Biochemistry and Molecular Medicine, Bern, Switzerland. [10]Present address: European Brain Research Institute, "Rita Levi-Montalcini" Foundation, Rome, Italy. [11]These authors contributed equally to this work. Correspondence should be addressed to G.M. (giovanni.marsicano@inserm.fr).

Received 11 November 2011; accepted 20 January 2012; published online 4 March 2012; doi:10.1038/nn.3053

membranes, and their direct activation regulates mitochondrial energetics. Furthermore, stimulation of intracellular CB_1 receptors and inhibition of presynaptic mitochondrial activity participate in endocannabinoid-dependent regulation of short-term synaptic plasticity in the hippocampus, providing a possible link between neuronal energy metabolism and specific neuronal functions.

RESULTS

CB_1 receptor protein is localized on neuronal mitochondria

CB_1 receptor immunoreactivity was detected by immunogold electron microscopy on mitochondrial membranes of CA1 hippocampal neurons of wild-type mice ($mtCB_1$; **Fig. 1a** and **Supplementary Fig. 1a**), but not *Cnr1*$^{-/-}$ (here called $CB_1^{-/-}$) littermates (**Fig. 1b** and **Supplementary Fig. 1b**). Approximately 30% of wild-type CA1 mitochondria displayed CB_1 immunolabeling, whereas only 2.9% ± 0.7% of CA1 mitochondria in $CB_1^{-/-}$ mice showed nonspecific labeling (**Fig. 1c**). $MtCB_1$ receptors were comparably distributed between axon terminals and somato-dendritic compartments in wild-type mice (**Supplementary Fig. 2a**). The density of $mtCB_1$ immunogold labeling was 18.3 ± 2.0 particles per μm^2 of mitochondria in wild type and dropped to 0.4 ± 0.1 particles per μm^2 in $CB_1^{-/-}$ mice (**Fig. 1d**). Further quantifications revealed that 15.5% ± 4.2% of CA1 neuronal total CB_1 protein was localized to mitochondria. Western immunoblotting confirmed the specific presence of CB_1 immunoreactivity in purified wild-type brain mitochondria (**Fig. 1e** and **Supplementary Fig. 3**). Semiquantification of immunogold images revealed that approximately 95% of $mtCB_1$ was localized to the outer membrane of mitochondria (**Fig. 1f**). This was confirmed by Western immunoblotting of purified mitochondria treated with trypsin with or without digitonin presolubilization, suggesting that the N-terminal portion of $mtCB_1$ is exposed to the cytosol, whereas the C terminus is likely located in the mitochondrial intermembrane space (**Fig. 1g** and **Supplementary Fig. 4**). Thus, a substantial portion of CB_1 receptor protein is present at the surface of neuronal mitochondria.

CB_1 receptors are expressed in different neuronal populations, where they negatively regulate excitability and neurotransmission[15–17]. These include inhibitory neurons containing GABA and excitatory glutamatergic neurons[24], where activation of CB_1 receptors differentially affects brain functions and behavior[16,17,27,28]. We analyzed the anatomical distribution of $mtCB_1$ receptors in the hippocampus of conditional mutant mice lacking CB_1 either in cortical glutamatergic (Glu-$CB_1^{-/-}$) or in GABAergic (GABA-$CB_1^{-/-}$) neurons, respectively[27,28]. $MtCB_1$ was still present in CA1 hippocampal neurons of both mutant strains (**Fig. 2a**,**b** and **Supplementary Fig. 1c**,**d**), with similar reductions in the percentage of labeled mitochondria relative to that in wild-type mice (**Fig. 2c**). In contrast, the density of $mtCB_1$ was reduced by 50.4% in GABA-$CB_1^{-/-}$, but not in Glu-$CB_1^{-/-}$, mutants (**Fig. 2d**). No difference between these two genotypes was observed concerning the proportion of $mtCB_1$ versus total CB_1 expression (**Fig. 2e**). As expected, most $mtCB_1$ was detected in terminals bearing asymmetric synapses (presumably excitatory) in GABA-$CB_1^{-/-}$ mice, whereas it was almost exclusively present on mitochondria of presumably inhibitory symmetric synapses in Glu-$CB_1^{-/-}$ mice (**Supplementary Fig. 2b**). Thus, both neuronal populations contain $mtCB_1$ receptors, which are, however, more densely expressed in hippocampal GABAergic neurons than in glutamatergic ones.

$MtCB_1$ directly regulates brain mitochondrial activity

The acute administration of THC to C57BL6/N mice (intraperitoneally, 5 mg per kilogram body weight) reduced mitochondrial

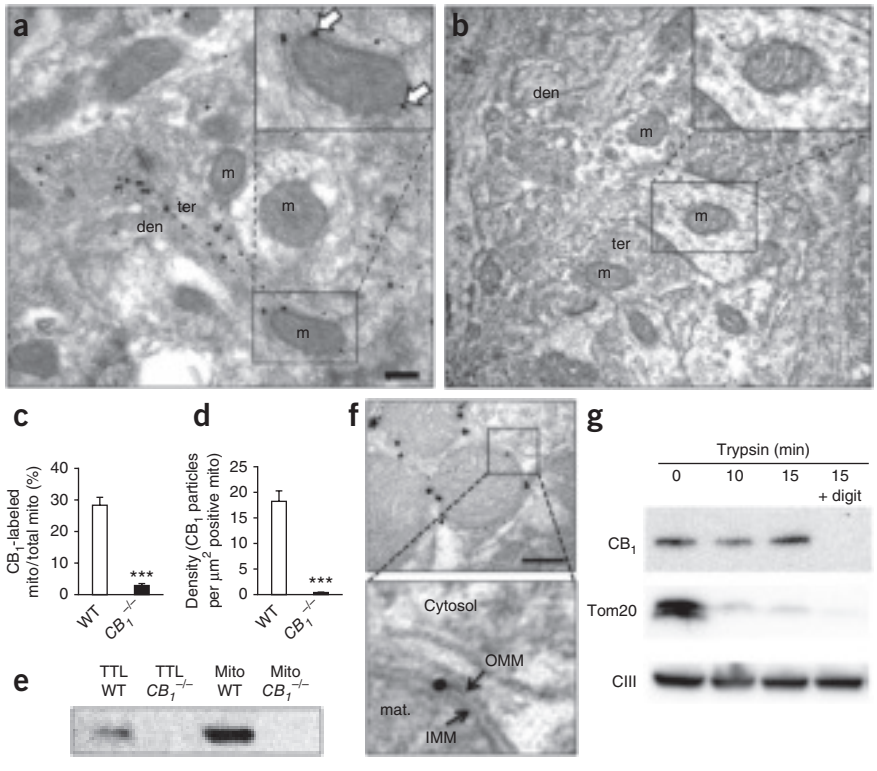

Figure 1 CB_1 receptors in neuronal mitochondria. (**a**,**b**) Electron immunogold detection of CB_1 receptors on mitochondrial membranes of neurons in the CA1 hippocampal region of wild-type (**a**) and $CB_1^{-/-}$ mice (**b**). Insets, details of single mitochondria. Arrows, specific CB_1 receptor localization. Scale bar, 200 nm. (**c**) CB_1-immunopositive mitochondria (mito) as a proportion of total mitochondria (WT, $n = 463$ mitochondria from 3 mice; $CB_1^{-/-}$, $n = 458$ mitochondria from 3 mice). (**d**) Density of CB_1 receptor immunoparticles per area of the immunopositive subset of mitochondria (WT, total mitochondrial area, 35.7 μm^2; $CB_1^{-/-}$, total mitochondrial area, 29.4 μm^2). (**e**) Immunoblotting of CB_1 receptor protein in whole brain total tissue lysate (TTL) from wild-type (WT) and $CB_1^{-/-}$ mice and purified mitochondria from WT and $CB_1^{-/-}$ mice. Full-length blots are shown in **Supplementary Figure 3c**. (**f**) Detail of CB_1 receptor gold particles on the outer mitochondrial membrane. Scale bar, 200 nm. (**g**) Trypsin and digitonin assay of CB_1 receptor expression in mitochondria. Resistance of $mtCB_1$ C-terminal domain to trypsin digestion but not to mild membrane permeabilization by digitonin (digit) indicates that the receptor is localized on the outer membrane with the C-terminal portion of the protein facing the mitochondrial intermembrane space. Full-length blots are shown in **Supplementary Figure 4**. Den, dendrites; ter, terminals; m, mitochondria; OMM, outer mitochondrial membrane; IMM, inner mitochondrial membrane; mat., matrix; Tom20, translocase of outer mitochondrial membranes 20 kDa; CIII, core 2 protein of mitochondrial complex III. Values, mean ± s.e.m. ***$P < 0.001$ as compared to WT.

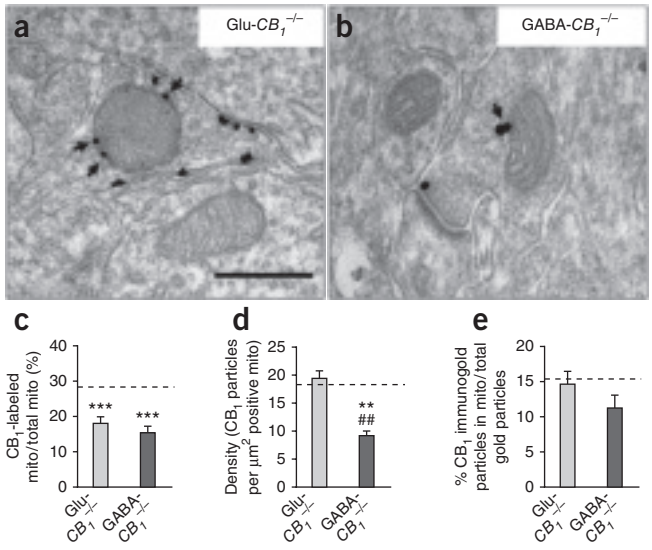

Figure 2 Mt-CB_1 is present in both GABAergic and glutamatergic CA1 hippocampal neurons. (**a**,**b**) Immunogold localization of mtCB_1 (arrows) in the CA1 hippocampal region of Glu-$CB_1^{-/-}$ (**a**) and GABA-$CB_1^{-/-}$ mice (**b**). (**c**) Proportion of CB_1-immunopositive mitochondria normalized to the total number of mitochondria in the CA1 hippocampal region of Glu-$CB_1^{-/-}$ ($n = 473$ mitochondria from 3 mice) and GABA-$CB_1^{-/-}$ mice ($n = 320$ mitochondria from 3 mice). (**d**) Density of mtCB_1 in Glu-$CB_1^{-/-}$ and GABA-$CB_1^{-/-}$ mice. (**e**) Proportion of mtCB_1 receptor normalized to the total CB_1 signal in the CA1 hippocampal region of Glu-$CB_1^{-/-}$ ($n = 31$ fields) and GABA-$CB_1^{-/-}$ ($n = 27$ fields) mice. Scale bar, 500 nm. Values, mean ± s.e.m. $^{**}P < 0.01$; $^{***}P < 0.001$ as compared to WT; $^{\#\#}P < 0.01$ as compared to Glu-$CB_1^{-/-}$ mice. Dashed horizontal lines, wild-type values.

respiratory chain complex I activity (particularly involved in neuronal bioenergetics)[4] in purified hippocampal mitochondria (vehicle, 94.7 ± 6.2; THC, 65.9 ± 8.1 nmol oxidized NADH per minute per milligram protein; $n = 6$, $P < 0.05$). CB_1 receptor signaling typically involves reduction of cAMP[15,19,29], and mitochondrial forms of adenylyl cyclase and protein kinase A (PKA) have been suggested to regulate complex I activity and mitochondrial respiration[7,8,11,13,14,30]. Acute THC treatment decreased mitochondrial cAMP by approximately 30% (vehicle, 0.60 ± 0.06; THC, 0.41 ± 0.06 nmol per mg protein; $n = 6$, $P < 0.05$). To test whether the effects of CB_1 receptor activation were due to a direct activation of mtCB_1 or to an indirect stimulation of CB_1 receptors located on the plasma membrane, brain mitochondria were purified from wild-type and $CB_1^{-/-}$ littermates (**Supplementary Fig. 3a**) and treated *in vitro* with the synthetic CB_1 agonist WIN55,212-2 (WIN). The drug dose-dependently decreased oxygen consumption in brain mitochondria from wild-type, but not $CB_1^{-/-}$, mice (**Fig. 3a**). WIN specifically decreased mitochondrial complex I activity (**Fig. 3b**) and cAMP content (**Fig. 3c**). Hippocampal neuronal mitochondria contained the A-kinase anchor protein 121 (AKAP121; **Supplementary Fig. 1e**), confirming that PKA activity occurs in these organelles[12]. WIN decreased mitochondrial PKA activity in an mtCB_1-dependent manner (**Fig. 3d**). To establish whether hippocampal CB_1 expression is sufficient for the mitochondrial effects of WIN, we injected the hippocampi of $CB_1^{-/-}$ mice with neurotropic adeno-associated viruses (AAV) expressing either a control protein (green fluorescent protein, AAV-GFP) or CB_1 (AAV-CB_1)[31]. The effect of WIN on complex I activity of purified hippocampal mitochondria was fully rescued by *in vivo* viral re-expression of the CB_1 receptor in $CB_1^{-/-}$ hippocampal mitochondria (**Fig. 3e**).

To investigate whether mtCB_1 is responsive to natural plant-derived cannabinoids, we measured the effects of THC on respiration, cAMP levels and PKA activity in neuronal mitochondria from wild-type and $CB_1^{-/-}$ littermates. THC induced effects similar to those of WIN (**Fig. 4a–c**), indicating that the functions of mtCB_1 are not dependent on the type of ligand.

Brain mitochondria have substantial levels of endocannabinoid degrading activity (**Supplementary Table 1**). To test whether endocannabinoids regulate mitochondrial activity *in situ*, we treated purified brain mitochondria with JZL195 (JZL), a dual inhibitor of fatty acid amide hydrolase (FAAH) and monoacylglycerol lipase (MAGL), the two main endocannabinoid degrading enzymes[15,32], and measured mitochondrial endocannabinoid levels and respiration. The endocannabinoid anandamide was detected in purified neuronal mitochondria, but its levels were below the limits of reliable quantification (data not shown). However, JZL dose-dependently increased mitochondrial 2-arachidonoylglycerol (**Fig. 4d**) and reduced respiration in brain mitochondria from wild-type, but not $CB_1^{-/-}$, mice (**Fig. 4e**). Notably, a highly significant inverse correlation was observed between 2-arachidonoylglycerol levels and mitochondrial respiration in wild-type brain mitochondria ($r = 0.82$, $P < 0.0001$; **Fig. 4f**).

Together, these data show that (i) mtCB_1 signaling directly affects mitochondrial cAMP accumulation, PKA activity, complex I activity and respiration in the brain, and (ii) mitochondria are equipped with endocannabinoids able to activate mtCB_1 *in situ*.

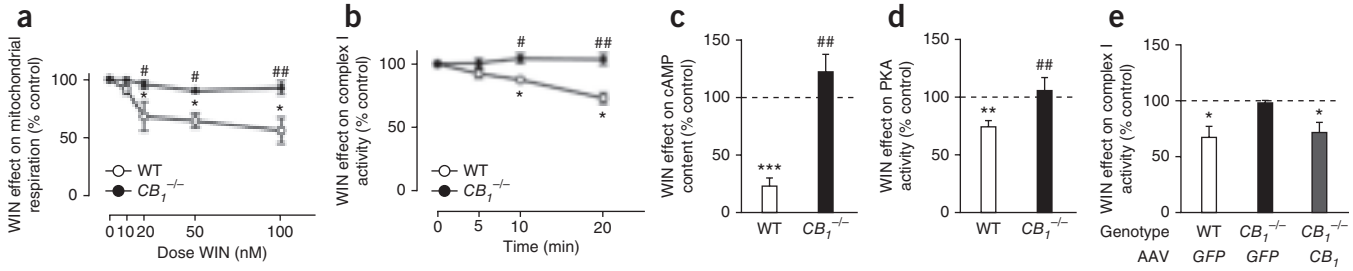

Figure 3 Direct regulation of mitochondrial activity by mtCB_1 receptors in the brain. (**a**) Dose–response curve for the effect of the CB_1 receptor agonist WIN on respiration of purified mitochondria from wild-type (WT) and $CB_1^{-/-}$ brains ($n = 4$ independent experiments). (**b**) Time course of enzymatic activity of complex I in the presence of 100 nM WIN in purified mitochondria from WT and $CB_1^{-/-}$ brains ($n = 3$). (**c**) cAMP content after 5 min treatment of purified mitochondria with 100 nM WIN ($n = 4$). (**d**) Effect of 100 nM WIN on mitochondrial PKA activity ($n = 3$). (**e**) Effect of 100 nM WIN on complex I activity in purified mitochondria from WT and $CB_1^{-/-}$ hippocampi locally injected with AAV-GFP, and from $CB_1^{-/-}$ hippocampi locally injected with AAV-CB_1 ($n = 6$ per group). Values, mean ± s.e.m. $^{*}P < 0.05$, $^{**}P < 0.01$; $^{***}P < 0.001$ as compared to control (vehicle or time 0); $^{\#}P < 0.05$, $^{\#\#}P < 0.01$ as compared to WT. Dashed horizontal lines, values for vehicle-treated controls.

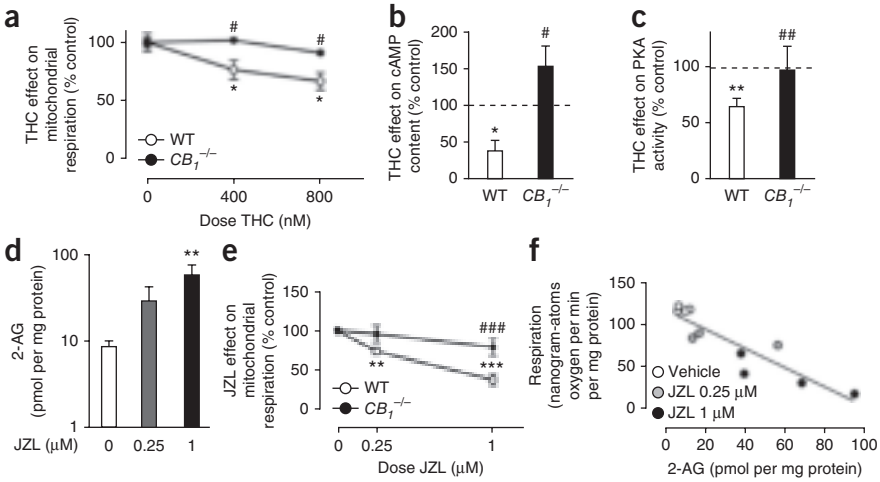

Figure 4 MtCB$_1$ receptors are activated by THC, and mitochondria contain biologically active endocannabinoids. (**a**) Dose–response curve for the effect of THC on respiration of purified mitochondria from wild-type (WT) and $CB_1^{-/-}$ brains. (**b**) Effect of THC on mitochondrial cAMP content in WT and $CB_1^{-/-}$ littermates. (**c**) Effect of THC on PKA activity in WT and $CB_1^{-/-}$ littermates. (**d**) Levels of the endocannabinoid 2-arachidonoylglycerol (2-AG) in purified brain mitochondria after treatment with the double MAGL and FAAH inhibitor JZL195 (JZL). Data are presented on a logarithmic scale (n = 3–5 pools of mitochondria purified each time from 10–15 mice). (**e**) Effect of JZL on respiration of purified brain mitochondria (n = 3–5 pools of mitochondria purified each time from 10–15 mice). (**f**) Correlation between 2-AG and respiration in purified brain mitochondria from WT mice (values are from **d**,**e**). Values, mean ± s.e.m. $^{*}P < 0.05$, $^{**}P < 0.01$, $^{***}P < 0.001$ as compared to vehicle control; $^{\#}P < 0.05$, $^{\#\#}P < 0.01$, $^{\#\#\#}P < 0.001$ as compared to WT. Dashed lines, vehicle values.

Intracellular CB$_1$ receptors participate in DSI

If mtCB$_1$ can control brain mitochondrial activity, are mitochondria involved in endocannabinoid-dependent neuronal functions? Retrograde control of hippocampal GABAergic transmission is an important endocannabinoid-dependent form of synaptic plasticity[15–17]. Depolarization of CA1 postsynaptic pyramidal neurons mobilizes endocannabinoids, which retrogradely activate presynaptic CB$_1$ receptors, transiently decreasing GABAergic inhibitory neurotransmission in a process known as depolarization-induced suppression of inhibition (DSI)[15–17]. DSI is blocked by CB$_1$ receptor antagonists and is occluded by CB$_1$ receptor agonists, which prevent the binding and the action of endogenously mobilized endocannabinoids[16]. If intracellular mtCB$_1$ receptors participate in the expression of DSI, cell-impermeant CB$_1$ receptor antagonists and agonists should not be able to fully block and occlude DSI, respectively. The peptide CB$_1$ receptor antagonist hemopressin[25,33,34] provided a first tool to test this hypothesis. As a peptide, hemopressin should not be able to penetrate plasma membranes[25]. This was confirmed both by measurements of intracellular fluorescence of cells treated with a fluorescent derivative of hemopressin (**Supplementary Fig. 5a–c**) and by spectrometric analysis of extracts from hippocampal slices incubated with hemopressin and the lipophilic CB$_1$ antagonist AM251 (**Supplementary Fig. 5d–f**). Thus, hemopressin can be used as a cell-impermeant CB$_1$ receptor antagonist.

To investigate the occluding effects of cell-impermeant CB$_1$ receptor agonists on DSI and to discriminate the relative influence of plasma membrane and intracellular CB$_1$ receptors on cellular respiration, we synthesized a biotinylated version of the lipophilic CB$_1$ receptor agonist HU210 (HU210-biotin, hereafter HU-biot). The presence of the hydrophilic biotin bulk should impede the cell penetration of this compound, and the presence of a spacer between the HU210 scaffold and the biotin moiety should preserve the affinity for CB$_1$ receptors. Radioligand competition experiments revealed that HU-biot displayed a comparable affinity for recombinant CB$_1$ receptors to that of HU210 (HU210, K_i = 0.2 ± 0.07 nM; HU-biot, K_i = 1.5 ± 0.4 nM). To characterize the ability of HU210 and HU-biot to penetrate plasma membranes and stimulate mtCB$_1$ receptors, we transfected primary mouse fibroblast cultures derived from $CB_1^{-/-}$ pups with a plasmid expressing the CB$_1$ receptor (creating MF-CB$_1$ cells). Neither HU210 nor HU-biot had any effect on cellular respiration of mock-transfected $CB_1^{-/-}$ mouse fibroblasts (**Fig. 5a**). Conversely, only HU210, but not HU-biot, decreased cellular respiration in MF-CB$_1$ cells (**Fig. 5b**), suggesting that cell penetration is a necessary step for this effect. Accordingly, HU-biot became as efficient as HU210 in depressing cell respiration in permeabilized MF-CB$_1$ cells (**Fig. 5c**), indicating that both drugs activate mtCB$_1$ receptors, but the difference relies on their cell permeance. Notably, hemopressin was not able to alter the effect of HU210 on intact MF-CB$_1$ cells (**Fig. 5b**), but it fully blocked this effect in permeabilized cells (**Fig. 5c**). These data indicate that (i) the lipophilic CB$_1$ agonist HU210 can penetrate cells and alter cellular respiration, (ii) HU-biot and hemopressin do not penetrate intact cells and do not alter cellular respiration, and, notably, (iii) only the activation of intracellular CB$_1$ receptors affects mitochondrial respiration of living cells.

We next analyzed the impact of the cell-permeant CB$_1$ antagonist AM251 and agonist HU210 on inhibitory synaptic transmission and DSI, and compared their effects to those of the cell-impermeant antagonist

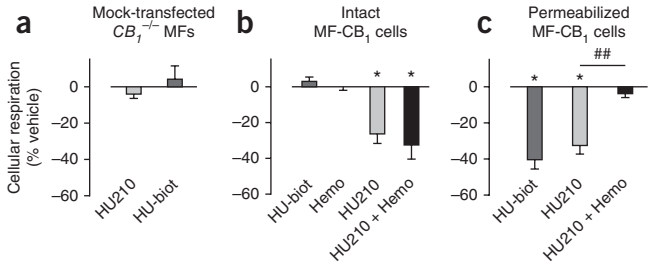

Figure 5 Hemopressin and HU-biot do not penetrate cells and cannot alter cellular respiration in intact cells. Mouse fibroblasts (MFs) were obtained from $CB_1^{-/-}$ pups and transfected with a vector expressing either the fluorescent protein mCherry (mock) or the CB$_1$ receptor (MF-CB$_1$). (**a**) Neither HU210 nor HU-biot altered cellular respiration in mock-transfected $CB_1^{-/-}$ MFs (n = 6 independent experiments). (**b**) HU-biot and hemopressin (Hemo) did not alter cellular respiration in MF-CB$_1$ cells, whereas the lipophilic agonist HU210 significantly decreased oxygen consumption. Hemo was not able to antagonize this effect of HU210 in intact MF-CB$_1$ cells (n = 4–7 independent experiments). (**c**) In permeabilized MF-CB$_1$ cells, HU-biot reduced cellular respiration and Hemo became able to fully block the depression by HU210 (n = 3–5 independent experiments). Values, mean ± s.e.m. $^{*}P < 0.05$ as compared to vehicle control. $^{\#\#}P < 0.01$.

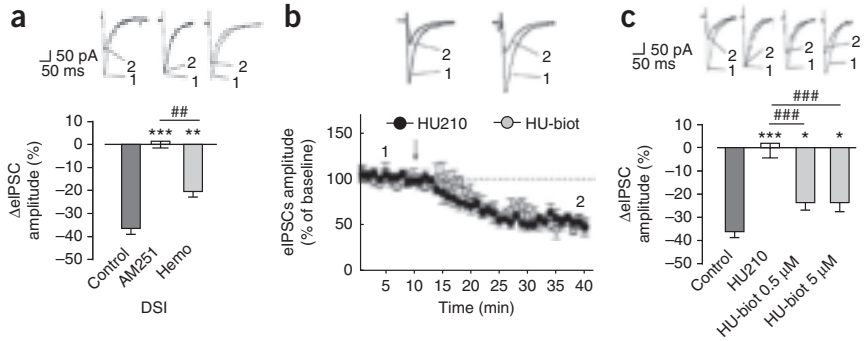

Figure 6 Intracellular CB_1 receptors contribute to depolarization-induced DSI. (**a**) Effects of the lipophilic CB_1 receptor antagonist AM251 (4 μM, $n = 5$ cells) and of the cell membrane–impermeant CB_1 receptor antagonist peptide hemopressin (Hemo, 10 μM; $n = 8$ cells) on the amplitude of strong DSI induced by a 5-s depolarization step from −70 to 0 mV of CA1 postsynaptic pyramidal neurons (Control, $n = 9$ cells). Top, representative electrophysiological traces (1 and 2, traces before and after depolarization, respectively); bottom, summary of results. (**b**) Effects of the lipophilic synthetic CB_1 receptor agonist HU210 (500 nM; $n = 7$ cells) and of the cell membrane–impermeant CB_1 receptor agonist HU-biot (500 nM; $n = 6$ cells) on normalized eIPSCs in CA1 pyramidal hippocampal neurons. Arrow, time of application of HU210 or HU-biot. Top, representative electrophysiological traces (1 and 2, traces before and after drug application, respectively); bottom, time course. (**c**) Occlusion effect of 30-min incubations of slices with HU210 ($n = 8$ cells) or with HU-biot at concentrations of 500 nM ($n = 7$ cells) or 5 μM ($n = 5$ cells) on the amplitude of strong DSI induced by a 5-s depolarization step of CA1 postsynaptic pyramidal neurons. Top, representative electrophysiological traces (1 and 2, traces before and after depolarization, respectively); bottom, summary of results. Values, mean ± s.e.m. $^{*}P < 0.05$, $^{**}P < 0.01$, $^{***}P < 0.0001$ as compared to control DSI. $^{\#\#}P < 0.01$; $^{\#\#\#}P < 0.001$.

hemopressin and agonist HU-biot, respectively. As expected[16], a 'strong' DSI induced by a 5-s depolarization of CA1 pyramidal neurons was fully blocked by AM251 (**Fig. 6a**). The application of hemopressin at a high dose (10 μM) did not alter evoked inhibitory postsynaptic currents (eIPSCs) when applied to hippocampal slices (**Supplementary Fig. 6a**,**b**). However, the peptide antagonist only partially and reversibly reduced DSI amplitude (**Fig. 6a** and **Supplementary Fig. 6c**,**d**). High concentrations of HU210 and HU-biot (500 nM) displayed a very similar ability to reduce eIPSCs (**Fig. 6b**), independently of the frequency of stimulation of afferent fibers (**Supplementary Fig. 6a**,**b**). Notably, the extracellular antagonist hemopressin fully blocked the depression of eIPSCs by both HU210 and HU-biot (**Supplementary Fig. 6a**,**b**), suggesting that intracellular CB_1 receptor signaling is not required for this pharmacological cannabinoid effect and that the biotin moiety does not alter the effect of HU210 on hippocampal GABAergic transmission. The maximal eIPSCs-depressing effect of both HU210 and HU-biot was observed after 25–30 min of incubation (**Fig. 6b** and **Supplementary Fig. 6a**). As expected, a 30-min incubation with HU210 fully occluded DSI induction in hippocampal slices (**Fig. 6c** and **Supplementary Fig. 6d**). In contrast, HU-biot only partially occluded DSI at concentrations of both 500 nM and 5 μM (**Fig. 6c** and **Supplementary Fig. 6d**). Thus, cell penetration of CB_1 antagonists and agonists is necessary for the respective full blockade and occlusion of DSI induced by 5-s depolarization of postsynaptic pyramidal neurons.

Inhibition of mitochondrial activity contributes to DSI

Rotenone is a well known specific and potent mitochondrial complex I inhibitor. The application of rotenone to hippocampal slices (2.5 μM) had no effect on strong DSI induced by a long depolarization period (5 s; **Fig. 7a**). However, if a weaker DSI was induced by a 1-s depolarization step, rotenone reliably enhanced DSI amplitude (**Fig. 7b**). Rotenone was unable to affect eIPSCs in the absence of depolarization (**Supplementary Fig. 7a**), to induce DSI in slices from $CB_1^{-/-}$ mice in the presence of the depolarization (**Supplementary Fig. 7b**), to alter the inhibitory effects of HU-biot on eIPSCs (**Supplementary Fig. 7c**), or to modify the levels of mitochondrial endocannabinoids (**Supplementary Fig. 7d**). These results indicate that the effect of rotenone on DSI was not due to a direct alteration of inhibitory neurotransmission, that it was dependent on CB_1 receptors, and that it was not due to increase in local endocannabinoid levels. DSI is mediated by presynaptic CB_1 receptors[16]. Rotenone did not

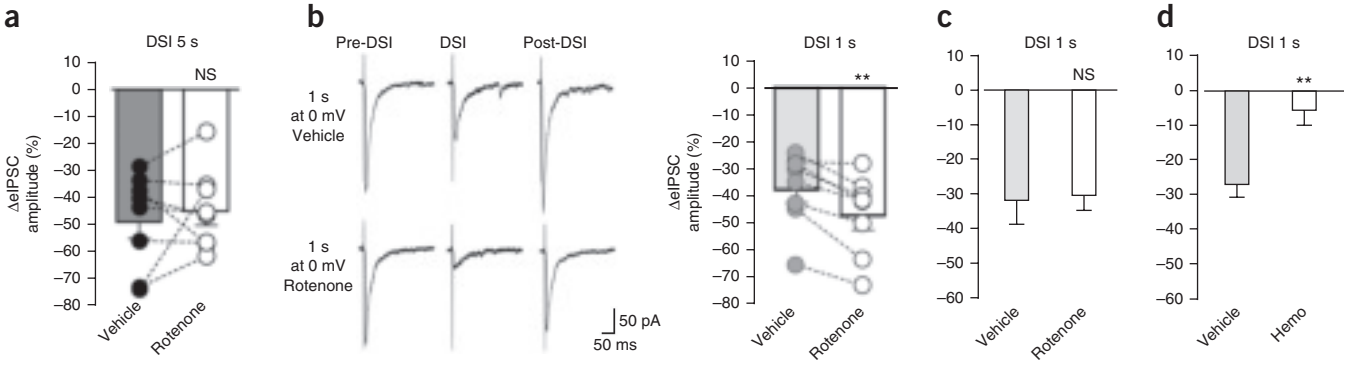

Figure 7 Inhibition of mitochondrial activity potentiates DSI. (**a**) Amplitudes of strong DSI induced by a 5-s depolarization step from −70 to 0 mV of CA1 postsynaptic pyramidal neurons before and after bath application of the mitochondrial complex I inhibitor rotenone (2.5 μM). (**b**) Amplitudes of weak DSI induced by a 1-s depolarization step of CA1 postsynaptic pyramidal neurons before and after bath application of rotenone (2.5 μM). Left, representative electrophysiological traces. Right, summary data plot. (**c**) Amplitude of DSI induced by a 1-s depolarization step of CA1 postsynaptic pyramidal neurons with postsynaptic intracellular application of vehicle ($n = 6$ cells) or rotenone (2.5 μM; $n = 6$ cells). (**d**) Effect of hemopressin (Hemo, 10 μM; $n = 7$ cells) on the amplitude of DSI induced by a 1-s depolarization step of CA1 postsynaptic pyramidal neurons (gray bar, $n = 7$ cells). Values, mean ± s.e.m. $^{**}P < 0.01$ as compared to control. NS, not significant.

produce any effect when infused postsynaptically (**Fig. 7c**), suggesting the involvement of presynaptic mitochondria in the expression of strong DSI. Consistent with these data, hemopressin was able to fully abolish a weak DSI induced by a 1-s depolarization (**Fig. 7d**), further confirming that intracellular CB_1 receptors contribute to strong, but not weak, forms of DSI.

DISCUSSION

The present results show that the CB_1 GPCR is present in a portion (approximately 30% in the hippocampus) of brain neuronal mitochondria, where it directly regulates mitochondrial respiration. This function may be exerted through the modulation of complex I activity, by regulating cAMP levels and PKA activity, which have been recently proposed to occur in mitochondria and to modulate the organelle's respiration and energy production[7,8,11,13,14,30]. Intracellular CB_1 receptors are involved in DSI, an endocannabinoid-dependent form of short-term plasticity of inhibitory neurotransmission in the hippocampus, and this function is mimicked by direct inhibition of complex I activity. Thus, these data establish the existence of $mtCB_1$ receptors and their role in the regulation of neuronal bioenergetics, which might be involved in endocannabinoid-dependent synaptic plasticity.

The hypothesis that GPCRs may directly regulate mitochondrial activity has been recently proposed[6,30]. The open source program MitoProt II (ref. 35) predicted the CB_1 receptor protein to bear a 39.3% probability of mitochondrial localization (**Supplementary Table 2**). This theoretical value is much higher than that of many GPCRs and is comparable to the values of several known or recently identified mitochondrial proteins (**Supplementary Table 2**). Our experimental data demonstrate that the metabotropic CB_1 receptor is present on mitochondrial membranes of neurons, where it acutely regulates energy metabolism and likely contributes to the expression of DSI.

The proportion of CB_1 receptors located on the mitochondrial membrane (approximately 15% of total cell CB_1 receptors) might seem low. However, this expression accounts for up to 30% of $mtCB_1$-dependent reduction of respiration in purified brain mitochondria. Notably, approximately 30% of neuronal mitochondria do contain CB_1 receptors, suggesting a strong impact of cannabinoid signaling on the subset of organelles expressing $mtCB_1$. Moreover, a low abundance of CB_1 receptors can bear crucial functional significance in specific locations. Although a minimal amount (less than 10%) of total cortical CB_1 receptor proteins are expressed in glutamatergic neurons[24,27], many of the functions of the endocannabinoid system are exerted by this limited percentage of receptors. For instance, protection against excitotoxic seizures or the orexigenic properties of endocannabinoid signaling are mainly exerted by glutamatergic-neuron CB_1 receptors[27,28]. Therefore, the 15% of hippocampal CB_1 protein located on mitochondrial membranes cannot be considered a negligible amount from a functional point of view.

Neuronal bioenergetics is emerging as a key player in brain functions[1,2,4,5]. This holds true for neurodegenerative disorders, in which mitochondrial alterations are thought to be of etiopathological relevance[4]. However, mitochondria also influence the normal functioning of the brain, regulating synaptic plasticity and possibly behavior[1,2,4,5]. The identification and functional characterization of brain $mtCB_1$ receptors provides a new mechanism of modulation of neuronal activity, which might have key roles in both physiological and pathological brain processes.

CB_1-dependent forms of synaptic plasticity such as DSI are likely to underlie many functions of endocannabinoid signaling in the brain[15–17]. Neurotransmitter release is a very energy-demanding process[5], and mitochondria can modulate its efficiency by different means[4]. The membrane-impermeant CB_1 receptor agonist HU-biot and the antagonist hemopressin only partially occluded and blocked DSI, respectively. In addition, inhibition of presynaptic mitochondrial activity by rotenone potentiated this form of synaptic plasticity, suggesting the involvement of mitochondrial activity in DSI. The latter effect could also be due to indirect effects of rotenone, which might potentiate endocannabinoid signaling by stimulation of neurotransmitter (for example, glutamate)[36] release, which can in turn increase endocannabinoid mobilization[16]. This is, however, unlikely because the application of rotenone postsynaptically or in the absence of postsynaptic depolarization did not alter inhibitory transmission. If rotenone were stimulating indirectly endocannabinoid mobilization *per se*, its application to slices should result into alterations of eIPSCs. Indeed, previous studies have shown that much higher concentrations of rotenone and much longer application periods are needed to alter synaptic transmission in the hippocampus[37]. Reduction of eIPSCs by exogenous application of cannabinoids does not seem to involve intracellular CB_1. Conversely, our data clearly show that intracellular CB_1 receptors (likely $mtCB_1$) participate in strong DSI. These apparently contradictory results suggest a mechanistic difference between the decrease of eIPSCs induced by exogenously applied cannabinoids or endogenously mobilized endocannabinoids. As yet, the mechanistic bases of this paradoxical difference are unknown, but they might rely on temporal and/or spatial aspects[17]. DSI is short-lasting (a few tens of seconds), likely due to efficient endogenous degradation of endocannabinoids[15,17]. Conversely, drug applications (especially of lipophilic cannabinoids) are generally long-lasting, their duration depending only on pharmacokinetics properties of the drug, and might induce extra effects (for example, tolerance)[29]. From the spatial point of view, the mobilization of endocannabinoids by depolarization and/or synaptic stimulation might be limited to specific cellular subdomains. Conversely, exogenous cannabinoids might display preference for other subdomains, thereby triggering different mechanisms. Finally, depolarization steps able to endogenously mobilize endocannabinoids might trigger other, so far unknown cellular events to favor additional means of endocannabinoid signaling, which would otherwise remain silent.

Taken together, our results show that intracellular CB_1 receptors participate in DSI and suggest that $mtCB_1$ might be the mediator of this intracellular endocannabinoid signaling. Endocannabinoids acting at presynaptic $mtCB_1$ receptors might contribute to DSI by temporarily decreasing mitochondrial respiration and altering the energy supply in the form of ATP needed for the ongoing release of neurotransmitters[4,5]. Moreover, mitochondria regulate intracellular calcium levels and redox potential, which can also modulate neuronal activity and neurotransmitter release[4]. Rapid trafficking of mitochondria has also been recently proposed to modulate synaptic plasticity[1], raising the possibility that $mtCB_1$ might interfere with these processes. Thus, $mtCB_1$ receptors might contribute to DSI and possibly to other forms of synaptic regulation and plasticity by different means.

The discovery that intracellular CB_1 receptor signaling and mitochondrial regulation are involved in DSI further extends the range of mechanisms through which endocannabinoid signaling influences brain functions and will possibly add new pharmacological targets for the therapeutic exploitation of the endocannabinoid system. The demonstration that CB_1 receptors are functionally expressed on neuronal mitochondria will pave the way for new studies investigating in deeper detail the relationship between GPCR signaling in the brain and cellular energy regulation, with unforeseeable effect on the development of new theoretical frameworks to better understand brain functioning in health and disease.

METHODS

Methods and any associated references are available in the online version of the paper at http://www.nature.com/natureneuroscience/.

Note: Supplementary information is available on the Nature Neuroscience website.

ACKNOWLEDGMENTS

We thank D. Gonzales, N. Aubailly and all the personnel of the Animal Facility of the NeuroCentre Magendie for mouse care and genotyping; all the members of G.M.'s laboratory for discussions; and A. Bacci, D. Cota, M. Guzman, U. Pagotto, P.V. Piazza and C. Wotjak for critically reading the manuscript. Supported by AVENIR/INSERM (G.M.), INSERM–Agence Nationale de la Recherche (Retour Post-Doc ANR-09RDPOC-006-01 (G.B.), European Union 7th Framework Program (REPROBESITY, HEALTH-F2-2008-223713, G.M. and B.L.), European Research Council (ENDOFOOD, ERC-2010-StG-260515, G.M.), Fondation pour la Recherche Medicale (G.M. and M.M.-L.), Region Aquitaine (G.M.), Fyssen Foundation (E.S.-G.), University of Bordeaux (J.L.), Red de Trastornos Adictivos, Instituto de Salud Carlos III (RD07/0001/2001, P.G.), Basque Country Government (GIC07/70-IT-432-07, P.G.), University of the Basque Country UPV/EHU (UFI11/41, P.G.), Comunidad de Madrid (S2010/BMD-2353, M.L.L.-R.), MICINN (SAF2009-07065, P.G.; SAF2010-22198-C02-01, M.L.L.-R.), Ramon y Cajal program (S.O.-G.), Deutsche Forschungsgemeinschaft (FOR926, B.L.) and CONACyT (E.S.-G.).

AUTHOR CONTRIBUTIONS

N.P., J.L. and L.B. equally contributed to experiments. P.G. and R.R. equally supervised different parts of this work. G.B., P.G., R.R. and G.M. designed the study. G.B. performed the biochemical experiments. F.M., J.L. and C.M. performed the electrophysiological studies. N.P. performed the anatomical studies. L.B. and E.S.-G. performed *in vivo* studies and stereotactic injections of viruses. A.D., M.M.-L., E.H.-C. and A.C. participated in biochemical experiments. I.M. measured endocannabinoids and endocannabinoid-degrading enzymatic activities. S.O.-G., M.M.-F. and M.L.L.-R. synthesized and biochemically characterized HU-biot and measured intracellular hemopressin and AM251. J.G. generated fluorescent hemopressin and performed *in vitro* studies on cell penetration. M.K., S.G. and B.L. provided the viruses for local re-expression of CB_1 receptors. F.C. supervised part of the work. P.G. supervised the anatomical studies. R.R. supervised biochemical experiments. G.M. conceived and supervised the whole study and wrote the manuscript. All authors edited the manuscript.

COMPETING FINANCIAL INTERESTS

The authors declare no competing financial interests.

Published online at http://www.nature.com/natureneuroscience/.
Reprints and permissions information is available online at http://www.nature.com/reprints/index.html.

1. MacAskill, A.F. & Kittler, J.T. Control of mitochondrial transport and localization in neurons. *Trends Cell Biol.* **20**, 102–112 (2010).
2. Attwell, D. & Laughlin, S.B. An energy budget for signaling in the grey matter of the brain. *J. Cereb. Blood Flow Metab.* **21**, 1133–1145 (2001).
3. Nicholls, D.G. & Ferguson, S.J. *Bioenergetics 3* (Academic Press, London, 2002).
4. Mattson, M.P., Gleichmann, M. & Cheng, A. Mitochondria in neuroplasticity and neurological disorders. *Neuron* **60**, 748–766 (2008).
5. Laughlin, S.B., de Ruyter van Steveninck, R.R. & Anderson, J.C. The metabolic cost of neural information. *Nat. Neurosci.* **1**, 36–41 (1998).
6. Belous, A.E. *et al.* Mitochondrial calcium transport is regulated by P2Y1- and P2Y2-like mitochondrial receptors. *J. Cell Biochem.* **99**, 1165–1174 (2006).
7. Lyssand, J.S. & Bajjalieh, S.M. The heterotrimeric G protein subunit G alpha i is present on mitochondria. *FEBS Lett.* **581**, 5765–5768 (2007).
8. Andreeva, A.V., Kutuzov, M.A. & Voyno-Yasenetskaya, T.A. G alpha12 is targeted to the mitochondria and affects mitochondrial morphology and motility. *FASEB J.* **22**, 2821–2831 (2008).
9. Zippin, J.H. *et al.* Compartmentalization of bicarbonate-sensitive adenylyl cyclase in distinct signaling microdomains. *FASEB J.* **17**, 82–84 (2003).
10. Acin-Perez, R. *et al.* A phosphodiesterase 2A isoform localized to mitochondria regulates respiration. *J. Biol. Chem.* **286**, 30423–30432 (2011).
11. Acin-Perez, R. *et al.* Cyclic AMP produced inside mitochondria regulates oxidative phosphorylation. *Cell Metab.* **9**, 265–276 (2009).
12. Ryu, H., Lee, J., Impey, S., Ratan, R.R. & Ferrante, R.J. Antioxidants modulate mitochondrial PKA and increase CREB binding to D-loop DNA of the mitochondrial genome in neurons. *Proc. Natl. Acad. Sci. USA* **102**, 13915–13920 (2005).
13. Chen, R., Fearnley, I.M., Peak-Chew, S.Y. & Walker, J.E. The phosphorylation of subunits of complex I from bovine heart mitochondria. *J. Biol. Chem.* **279**, 26036–26045 (2004).
14. Helling, S. *et al.* Phosphorylation and kinetics of mammalian cytochrome c oxidase. *Mol. Cell Proteomics* **7**, 1714–1724 (2008).
15. Piomelli, D. The molecular logic of endocannabinoid signalling. *Nat. Rev. Neurosci.* **4**, 873–884 (2003).
16. Kano, M., Ohno-Shosaku, T., Hashimotodani, Y., Uchigashima, M. & Watanabe, M. Endocannabinoid-mediated control of synaptic transmission. *Physiol. Rev.* **89**, 309–380 (2009).
17. Marsicano, G. & Lutz, B. Neuromodulatory functions of the endocannabinoid system. *J. Endocrinol. Invest.* **29**, 27–46 (2006).
18. Bartova, A. & Birmingham, M.K. Effect of delta9-tetrahydrocannabinol on mitochondrial NADH-oxidase activity. *J. Biol. Chem.* **251**, 5002–5006 (1976).
19. Matsuda, L.A., Lolait, S.J., Brownstein, M.J., Young, A.C. & Bonner, T.I. Structure of a cannabinoid receptor and functional expression of the cloned cDNA. *Nature* **346**, 561–564 (1990).
20. Martin, B.R. Cellular effects of cannabinoids. *Pharmacol. Rev.* **38**, 45–74 (1986).
21. Tedesco, L. *et al.* Cannabinoid receptor stimulation impairs mitochondrial biogenesis in mouse white adipose tissue, muscle, and liver: the role of eNOS, p38 MAPK, and AMPK pathways. *Diabetes* **59**, 2826–2836 (2010).
22. Aquila, S. *et al.* Human sperm anatomy: ultrastructural localization of the cannabinoid1 receptor and a potential role of anandamide in sperm survival and acrosome reaction. *Anat. Rec. (Hoboken)* **293**, 298–309 (2010).
23. Gulyas, A.I. *et al.* Segregation of two endocannabinoid-hydrolyzing enzymes into pre- and postsynaptic compartments in the rat hippocampus, cerebellum and amygdala. *Eur. J. Neurosci.* **20**, 441–458 (2004).
24. Marsicano, G. & Kuner, R. Anatomical distribution of receptors, ligands and enzymes in the brain and the spinal cord: circuitries and neurochemistry. in *Cannabinoids and the Brain* (ed. Kofalvi, A.) 161–202 (Springer, New York, 2008).
25. Rozenfeld, R. & Devi, L.A. Regulation of CB1 cannabinoid receptor trafficking by the adaptor protein AP-3. *FASEB J.* **22**, 2311–2322 (2008).
26. Marsicano, G. *et al.* The endogenous cannabinoid system controls extinction of aversive memories. *Nature* **418**, 530–534 (2002).
27. Bellocchio, L. *et al.* Bimodal control of stimulated food intake by the endocannabinoid system. *Nat. Neurosci.* **13**, 281–283 (2010).
28. Monory, K. *et al.* The endocannabinoid system controls key epileptogenic circuits in the hippocampus. *Neuron* **51**, 455–466 (2006).
29. Pertwee, R.G. Pharmacology of cannabinoid receptor ligands. *Curr. Med. Chem.* **6**, 635–664 (1999).
30. Papa, S. Does cAMP play a part in the regulation of the mitochondrial electron transport chain in mammalian cells? *IUBMB Life* **58**, 173–175 (2006).
31. Guggenhuber, S., Monory, K., Lutz, B. & Klugmann, M. AAV vector-mediated overexpression of CB1 cannabinoid receptor in pyramidal neurons of the hippocampus protects against seizure-induced excitoxicity. *PLoS ONE* **5**, e15707 (2010).
32. Long, J.Z. *et al.* Dual blockade of FAAH and MAGL identifies behavioral processes regulated by endocannabinoid crosstalk in vivo. *Proc. Natl. Acad. Sci. USA* **106**, 20270–20275 (2009).
33. Heimann, A.S. *et al.* Hemopressin is an inverse agonist of CB1 cannabinoid receptors. *Proc. Natl. Acad. Sci. USA* **104**, 20588–20593 (2007).
34. Gomes, I. *et al.* Hemoglobin-derived peptides as novel type of bioactive signaling molecules. *AAPS J.* **12**, 658–669 (2010).
35. Claros, M.G. & Vincens, P. Computational method to predict mitochondrially imported proteins and their targeting sequences. *Eur. J. Biochem.* **241**, 779–786 (1996).
36. Kilbride, S.M., Telford, J.E., Tipton, K.F. & Davey, G.P. Partial inhibition of complex I activity increases Ca-independent glutamate release rates from depolarized synaptosomes. *J. Neurochem.* **106**, 826–834 (2008).
37. Costa, C. *et al.* Electrophysiology and pharmacology of striatal neuronal dysfunction induced by mitochondrial complex I inhibition. *J. Neurosci.* **28**, 8040–8052 (2008).

ONLINE METHODS

Mice. Experiments were approved by the Committee on Animal Health and Care of INSERM and the French Ministry of Agriculture and Forestry (authorization number 3306369). Mice were maintained under standard conditions. Female mice (2–4 months old) were used for anatomy and biochemistry. Mice 20–30 d old of both sexes were used for electrophysiology. $CB_1^{-/-}$, Glu-$CB_1^{-/-}$ and GABA-$CB_1^{-/-}$ mice (elsewhere called CB_1-KO, Glu-CB_1-KO and GABA-CB_1-KO, respectively) were as described[26–28,38,39]. C57BL/6N were from Janvier (France). Experimenters were blind to genotypes and treatments. A total of 312 female and 22 male mice were used.

Drugs. Drugs were from Sigma, Tocris, Abbott Laboratories Inc. or Ascent Scientific. THC was dissolved in ethanol; WIN55,252-2 (WIN), HU210 and HU-biot (see below) in DMSO; hemopressins in PBS. Vehicles contained the same amounts of solvents (0.1–0.2% ethanol; 0.1% DMSO).

Synthesis of and CB_1 binding assay for HU-biot. HU-biot was prepared by condensation between HU210 (ref. 40) and *N*-(+)-biotinyl-6-aminohexanoic acid in the presence of dicyclohexylcarbodiimide, *N*,*N*-dimethylaminopyridine and *N*-hydroxybenzotriazole as coupling reagents (yield: 32%) and purified by column chromatography. Spectroscopic data were consistent with the structure. Purity (elemental analysis) > 95%. The CB_1 binding assay was performed as previously described[41].

Synthesis of fluorescent hemopressin. Rat hemopressin was synthesized using standard Fmoc solid-phase synthesis chemistry on a CS336S Peptide Synthesizer (CS Bio Co.). 5 mg ml^{-1} hemopressin in PBS (pH 7.2) containing 5 mM tris (2-carboxyethyl)phosphine hydrochloride (Pierce) were incubated (20 min at room temperature) and incubated (2 h, room temperature) with a 10 mg ml^{-1} solution of maleimide-activated mcKLH carrying an succinimidyl-4-(*N*-maleimidomethyl)-cyclohexane-1-carboxylate (SMCC) crosslinker (Pierce). The final peptide–protein carrier conjugate was purified, concentrated and analyzed with SDS-PAGE following Coomassie brilliant blue G-250 staining. The introduction of fluorescein to the peptide was done by a one-step procedure coupling fluorescein-5-maleimide (Pierce) to the cysteine. The product was reconstituted in DMSO and purified and analyzed with preparative HPLC and ESI-MS.

CB_1 binding assay with fluorescent hemopressin. The K_d value of the fluorescent hemopressin was determined using CHO-K1 cells expressing human CB_1 (hCB_1). The peptide was incubated with 1×10^5 cells suspended in 200 µl binding buffer (50 mM Tris-HCl, 2.5 mM EDTA, 5 mM $MgCl_2$, 0.5% BSA, pH 7.4) in silanized plastic tubes (30 min, 30 °C). After centrifugation and three washes with ice-cold binding buffer, fluorescence intensities were measured in a 96-well plate reader (Tecan Farcyte, 485-nm excitation and 535-nm emission). Specific binding was determined after washing and subtracting of signals from untransfected control cells. Concentration response curves were analyzed by nonlinear curve fitting (one-site binding). The apparent K_d value for the CB_1 receptor was 119 ± 11 nM.

Immunocytochemistry for electron microscopy. Wild-type, Glu-$CB_1^{-/-}$, GABA-$CB_1^{-/-}$ and $CB_1^{-/-}$ mice (n = 3 each) were processed for electron microscope pre-embedding immunogold labeling as recently described[42]. Antibodies used in 50-µm-thick hippocampal sections: goat CB_1 antiserum (2 µg ml^{-1}; CB1-Go-Af450-1, Frontier Science Co. Ltd); goat AKAP 121 antiserum (2 µg ml^{-1}; AKAP 149/121, Santa Cruz Biotechnology).

Semiquantification of mtCB1. The detailed procedure has been described elsewhere[42]. The number of labeled mitochondria normalized to total mitochondria determined the proportion of hippocampal CA1 CB_1-immunopositive mitochondria. MtCB_1 labeling density was calculated on the area of labeled mitochondria. Normalized mtCB_1 labeling versus total CB_1 showed mtCB_1 proportion versus total CB_1. Axon terminals identification: abundant synaptic vesicles, mitochondria, synapses with dendritic elements. No difference in percentage of labeled mitochondria, in density of mtCB_1 or proportion of mtCB_1 versus total CB_1 was observed between the wild-type littermates of the different mutant mice ($P > 0.6$, for each parameter, one-way ANOVA), allowing the pooling of respective wild-type littermate controls. Normalized CA1 asymmetric or symmetric terminals with mtCB1 versus total asymmetric or symmetric synaptic boutons containing mitochondria revealed the percentages of axon terminals containing mtCB1 in Glu-$CB_1^{-/-}$ and GABA-$CB_1^{-/-}$ mice.

Cell culture and transfection. Mouse primary fibroblasts (MFs) were generated from P0–P1 $CB1^{-/-}$ mice. Dorsal skin was excised and minced in PBS and then incubated with in 0.25% trypsin solution. Cells were collected by centrifugation and resuspended in DMEM with 10% FBS, 1% L-glutamine and 2% penicillin/streptomycin solution (Invitrogen). Cells were seeded onto 25-cm^2 flasks. Transfections were carried out by using a BTX electroporator ECM 830 (Harvard apparatus, 175V, 1-ms pulse, five pulses, 0.5-s interval between pulses). Cell were electroporated in Optimem medium (Invitrogen) at 2×10^7 cells ml^{-1} in a 2-mm-gap cuvette using 30 µg of DNA. After electroporation, cells were resuspended in culture medium and experiments were performed 3 d later.

Mitochondrial purification from mouse hippocampi or whole brain. After death, the brains or hippocampi of $CB_1^{-/-}$ and wild-type littermates were dissected and mitochondria were purified as previously described[43].

Trypsin and digitonin assays. Mitochondria diluted in isolation buffer (100 µg) were treated or not with digitonin (0.25%, w/v, room temperature, 15 min). Trypsin digestion (0.1% w/v) was performed for 0, 5, 10 or 15 min (room temperature). The reaction was stopped by adding protease inhibitor cocktail (Roche). All samples were centrifuged (12,000*g*, 4 °C, 10 min). Each pellet was suspended in sample buffer and analyzed by western blot.

Oxygen consumption assays. Oxygen consumption was monitored at 30 °C in a glass chamber equipped with a Clark oxygen electrode (Hansatech). Purified mitochondria (1 mg) were suspended in 1 ml of the respiration buffer (75 mM mannitol, 25 mM sucrose, 10 mM KCl, 10 mM Tris-HCl, pH 7.4, 50 mM EDTA) in the chamber. Respiratory substrates (10 mM pyruvate and malate) were added directly to the chamber. A coupled respiratory state was obtained by adding 2 mM ADP.

The experiments using MFs were performed on 2×10^6 cells ml^{-1} in growth medium. Intact cells were transferred directly in the chamber and respiration was recorded. For experiments with permeabilized cells, MFs were supplemented with respiratory substrates (10 mM pyruvate and malate) and 2 mM ADP and permeabilized with digitonin (20 µg ml^{-1}).

The effects of hemopressin, WIN, JZL195, HU210 and HU-biot were analyzed by adding the drugs directly to the chamber.

NADH-ubiquinone oxidoreductase (complex I) activity assay. We followed the reaction of NADH oxidation into NAD^+ by complex I as previously described[43].

Immunoblotting. All samples were supplemented with proteases inhibitors (Roche) and diluted in sample buffer. Samples were supplemented with 2% beta-mercaptoethanol and 50 mM DTT and boiled for ~5 min. Nonreducing conditions (beta-mercaptoethanol and DTT omitted) were also used in some experiments (**Supplementary Fig. 3b**). Proteins were separated on Tris-glycine 4–16% acrylamide gels and transferred to PVDF membranes. Membranes were soaked in 5% milk in PBS-Tween20 (0.05%). Mitochondrial proteins were immunodetected using antibodies against complex III (Mitosciences, 2 h, room temperature) and Tom-20 (Santa Cruz, overnight, 4 °C). Cytosol, endoplasmic reticulum (ER), synaptosomes and plasma membrane contaminations were investigated using antibodies respectively against GAPDH (Santa Cruz, overnight, 4 °C), calreticulin (Santa Cruz, overnight, 4 °C), KDEL (ER; Enzo Life Sciences, 1 h, room temperature), synaptophysin (Millipore, 2 h, room temperature) and cadherin (Santa Cruz, overnight, 4 °C). The presence of the CB_1 in mitochondrial fractions was analyzed using an antiserum directed against the C terminus of the receptor (Cayman, overnight, 4 °C). Then membranes were washed and incubated with secondary HRP-coupled antibodies (1 h, room temperature). Finally, HRP signal was revealed using the ECL plus reagent (Amersham) and detected by the Bio-Rad Quantity One system.

Cyclic AMP and PKA activity assays. Cyclic AMP activity and PKA activities were assayed on isolated mitochondria using the Direct Correlate-EIA cAMP kit (Assay Designs Inc) and an ELISA kit (Enzo Life Science), respectively, according to the manufacturers' instructions. Reactions in presence or absence of WIN or THC were performed at 30 °C for 1 h.

Purification and quantification of endocannabinoids and *N*-acylethanolamides. Purification and quantification of anandamide, 2-arachidonoylglycerol (2-AG), palmitoylethanolamide and oleoylethanolamide from the brain total membrane fraction and purified mitochondria were performed as described previously[44]. The amounts of anandamide and 2-AG were determined using a calibration curve and were expressed as nmol or pmol per mg of protein, respectively. Anandamide was detected in the samples, but at levels below the limit of reliable quantification. Therefore, only data relating to 2-AG are presented.

Fatty acid amide hydrolase and monoacylglycerol lipase assays. FAAH or MAGL activities were detected by using brain total membrane fraction or purified mitochondria (50 µg protein), and [^{14}C]anandamide (for FAAH, 5.0 mCi mmol^{-1}, 1.8 µM, ARC Inc.) or 2-oleoyl-[^{3}H]glycerol (for MAGL, 1.0 mCi mmol^{-1}, 25 µM, ARC Inc.) as substrates. Reactions were carried out in 50 mM Tris-HCl, pH 9 (30 min, 37 °C) for FAAH and in Tris-HCl buffer, pH 7 (20 min, 37 °C) for FAAH and MAGL, respectively. The [^{14}C]ethanolamine (for FAAH) or [^{3}H]glycerol (for MAGL) produced were measured by scintillation counting of the aqueous phase after extraction of the incubation mixture with 2 volumes of $CHCl_3$/CH_3OH (1:1 v/v). Enzymatic activities were expressed as pmol of hydrolyzed anandamide or 2-AG per min per mg protein.

Viral rescue of CB1 expression in the hippocampus. Cloning of hemagglutinin (HA)-tagged rat CB_1 receptor (AAV-CB_1) or green fluorescent protein (AAV-GFP) into an AAV expression cassette, packaging of AAV1/2 chimeric vectors and determination of genomic titers were as described[31,45]. One µl of either AAV-GFP or AAV-CB1 (6×10^{11} viral genomes ml^{-1}) was injected bilaterally at 150 nl min^{-1} into the dorsal and ventral hippocampus (−2.0 mm AP, ± 2.0 mm ML, −2.0 mm DV; −3.5 mm AP, ± 3.4 mm ML, −3.0 mm DV from bregma, respectively). Animals were used for experiments five weeks after viral injection[31].

Cellular localization of fluorescent hemopressin. 1×10^6 hCB_1-expressing CHO-K1 cells were incubated with 10 µM fluorescent hemopressin in 50 mM Tris-HCl, pH 7.4, 2.5 mM EDTA and 5 mM $MgCl_2$ (30 min, 30 °C), washed different times (**Supplementary Fig. 4a–c**) in incubation buffer plus 0.5% BSA, detached with trypsin, and fixed with 0.01% formaldehyde (10 min). Fluorescence was measured by flow cytometry (FACScan, Cytek). Some cells were permeabilized with 0.5% NP-40 in PBS before incubation. Images were acquired with a Nikon TS100 fluorescence microscope and video camera using the NIS Elements D software.

Measurement of hemopressin and AM251 by liquid chromatography/mass spectrography. Slices previously incubated with 10 µM hemopressin or AM251 (same conditions as in electrophysiology experiments) were rinsed with water, centrifuged, Dounce-homogenized in chloroform:methanol:water (2:1:1; 2 ml), and the organic and aqueous layers separated by centrifugation. For hemopressin, the aqueous phase was dried under a stream of argon and reconstituted in 100 µL H_2O, and 60 µL were analyzed by LC/MS. For AM251, the organic phase was dried under a stream of argon and reconstituted in 100 µL of acetonitrile, and 50 µL were analyzed by LC/MS. LC/MS was carried out in an Agilent 1200LC-MSD VL instrument with an Eclipse XDB-C18 column coupled to an ESI source in SIM mode. The mobile phases were A (95:5 water:methanol) and B (95:5 methanol:water) with 0.1% ammonium hydroxide and 0.1% formic acid. Fractions were quantified by measuring the area under the peak and compared to corresponding standards.

Electrophysiology. Preparation of hippocampal slices and recording of eIPSCs were as previously described[28,46]. After reaching stable baseline (~10 min after reaching whole-cell configuration for infusion of intracellular solution), IPSCs were evoked using a patch pipette filled with a HEPES-based extracellular solution positioned in the stratum radiatum, 100 µm from the CA1 pyramidal cell layer. DSI expression was checked before starting each experiment with a 5-s depolarization protocol[46]. Control experiments showed that this 'initial' DSI had no effect on following recorded DSI (not shown).

To determine the effects of HU210 (500nM), HU-biot (500nM) and rotenone (2.5 µM) on basal inhibitory synaptic transmission, IPSCs were evoked every 10–15 s. To determine the effects of HU210, HU-biot, hemopressin (10 µM) and rotenone on basal inhibitory synaptic transmission using the same conditions of afferent stimulation as during DSI protocols (see below), IPSCs were evoked every 3 s and a stable baseline was recorded (time 0). Then, drugs (or vehicle) were applied and patched cells were left undisturbed. The same stimulation protocol was then applied every 10 min after drug applications up to 30 min.

For DSI, IPSCs were evoked every 3 s, and DSI was induced by a 1-s or a 5-s voltage step from −70 to 0 mV applied to the postsynaptic pyramidal neuron and calculated as described[46].

Two different treatment schemes were used to evaluate the effect of the different drugs on DSI. In some experiments (**Fig. 6a**,**c** and **7d**), slices were first incubated with drugs (or vehicle) for 30 min. A CA1 pyramidal cell was then patched and, after a stable baseline was obtained, a DSI protocol was applied. In other experiments (**Fig. 7a–c** and **Supplementary Figs. 6a–c** and **7b**,**c**), a pairwise schedule was used: CA1 pyramidal neurons were patched and, after we obtained a stable baseline, a DSI protocol was applied. Then, drugs were applied and a new DSI protocol was applied after 15 min of baseline recording. The effect of postsynaptic rotenone on DSI was studied by adding the drug (2.5 µM) to the intracellular solution in the patch pipette.

Statistical analyses. All graphs and statistical analyses were performed using GraphPad software (version 5.0). Results were expressed as means of independent data points ± s.e.m. Data were analyzed using a paired or unpaired Student's *t*-test, one-way ANOVA (followed by Newman-Keuls *post hoc* test), or two-way ANOVA (followed by Bonferroni's *post hoc* test), as appropriate.

38. Marsicano, G. *et al.* CB1 cannabinoid receptors and on-demand defense against excitotoxicity. *Science* **302**, 84–88 (2003).
39. Monory, K. *et al.* Genetic dissection of behavioural and autonomic effects of Delta(9)-tetrahydrocannabinol in mice. *PLoS Biol.* **5**, e269 (2007).
40. Mechoulam, R., Lander, N., University, A. & Zahalka, J. Synthesis of the individual, pharmacologically distinct, enantiomers of a tetrahydrocannabinol derivative. *Tetrahedron Asymmetry* **1**, 315–318 (1990).
41. Martín-Couce, L., Martín-Fontecha, M., Capolicchio, S., López-Rodríguez, M.L. & Ortega-Gutiérrez, S. Development of endocannabinoid-based chemical probes for the study of cannabinoid receptors. *J. Med. Chem.* **54**, 5265–5269 (2011).
42. Puente, N. *et al.* Polymodal activation of the endocannabinoid system in the extended amygdala. *Nat. Neurosci.* **14**, 1542–1547 (2011).
43. Benard, G. *et al.* Physiological diversity of mitochondrial oxidative phosphorylation. *Am. J. Physiol. Cell Physiol.* **291**, C1172–C1182 (2006).
44. Lourenço, J., Matias, I., Marsicano, G. & Mulle, C. Pharmacological activation of kainate receptors drives endocannabinoid mobilization. *J. Neurosci.* **31**, 3243–3248 (2011).
45. Klugmann, M. *et al.* AAV-mediated hippocampal expression of short and long Homer 1 proteins differentially affect cognition and seizure activity in adult rats. *Mol. Cell Neurosci.* **28**, 347–360 (2005).
46. Lourenço, J. *et al.* Synaptic activation of kainate receptors gates presynaptic CB(1) signaling at GABAergic synapses. *Nat. Neurosci.* **13**, 197–204 (2010).

doi:10.1038/nn.3053